Super-resolution reconstruction algorithm for terahertz imaging below diffraction limit

Ying Wang(王莹)[1,2,3,4], Feng Qi(祁峰)[2,3,4,5,†], Zi-Xu Zhang(张子旭)[6], and Jin-Kuan Wang(汪晋宽)[1]

[1] *School of Communication Science and Engineering, Northeastern University, Shenyang* 110819, *China*
[2] *Key Laboratory of Opto-Electronic Information Processing, Chinese Academy of Sciences, Shenyang* 110016, *China*
[3] *Shenyang Institute of Automation, Chinese Academy of Sciences, Shenyang* 110016, *China*
[4] *Institutes for Robotics and Intelligent Manufacturing, Chinese Academy of Sciences, Shenyang* 110169, *China*
[5] *University of Chinese Academy of Sciences, Beijing* 100049, *China*
[6] *University of Technology Sydney, NSW* 2007, *Australia*

(Received 13 October 2022; revised manuscript received 25 November 2022; accepted manuscript online 8 December 2022)

Terahertz (THz) imaging has drawn significant attention because THz wave has a unique capability to transient, ultra-wide spectrum and low photon energy. However, the low resolution has always been a problem due to its long wavelength, limiting their application of fields practical use. In this paper, we proposed a complex one-shot super-resolution (COSSR) framework based on a complex convolution neural network to restore superior THz images at 0.35 times wavelength by extracting features directly from a reference measured sample and groundtruth without the measured PSF. Compared with real convolution neural network-based approaches and complex zero-shot super-resolution (CZSSR), COSSR delivers at least 6.67, 0.003, and 6.96% superior higher imaging efficacy in terms of peak signal to noise ratio (PSNR), mean square error (MSE), and structural similarity index measure (SSIM), respectively, for the analyzed data. Additionally, the proposed method is experimentally demonstrated to have a good generalization and to perform well on measured data. The COSSR provides a new pathway for THz imaging super-resolution (SR) reconstruction below the diffraction limit.

Keywords: terahertz, image processing, complex convolution neural network

PACS: 87.50.U–, 87.85.dq, 95.75.Mn **DOI:** 10.1088/1674-1056/aca9c7

1. Introduction

Since THz waves possess unique properties,[1,2] their application in imaging has been a hot topic for years. THz imaging[3,4] contains numerous spectrum information and is a good tradeoff between penetration and resolution in imaging applications.[5–12] Although THz waves have a pronounced diffraction effect and a longer wavelength than optics, they still pose a resolution bottleneck. Getting half-wavelength resolution is not easy, and only those with delicate THz optical components and excellent alignment can achieve it. The resolution is usually in the order of wavelength instead of sub-wavelength, not to mention the diffraction limit.

Deep learning is an emerging data analysis and processing tool with the unique advantage of learning the intrinsic laws of data and input–output mapping relationships. During the past decade, convolution neural network (CNN)[13] has been verified to improve the resolution in optical imaging[14–18] with real numbers corresponding to recorded intensity for calculations. In recent years, an adaptation of deep learning for THz imaging SR reconstruction has received remarkable attention from researchers. Various researchers have successfully demonstrated how deep learning can improve the resolution of the THz image[19–21] for many applications, including medical diagnosis, non-destructive inspection, and safety inspection. The classical CNN SR algorithms rely on geometrical optics, and phase operations are not implemented since most optical facilities cannot directly measure phase. THz is a kind of wave that is quite feasible to gain amplitude and phase information.

Wei Ning *et al.*[22] extend CLS deconvolution to a complex domain, which has verified that useful information could be extracted from phase images to improve the resolution of the terahertz image. Based on this concept, we extend the calculations in CNN from the real number domain to the complex number domain by taking the physical nature of the THz wave. In our previous research,[23] we proposed a THz image super-resolution based on a complex convolution neural network (CCNN). Such a CCNN is successful in THz imaging for the first time. Compared to CNN, the quality of the reconstructed image has been improved obviously by using CCNN in terms of contrast, entropy, *etc*. Moreover, CCNN has better generalization abilities so that phase information can be recovered accurately, which is impossible to achieve in classical CNN. A complex zero-shot super-resolution reconstruction (CZSSR)[24] algorithm based on internal image statistics is proposed to address the issue of THz SR algorithms without standard training datasets. Instead of relying on pre-training, the proposed method is of sound self-adaptability. The resolution of these methods has reached the theoretical limit of half a wavelength. Physically, the resolution is only 0.4 times the

[†]Corresponding author. E-mail: qifeng@sia.cn

© 2023 Chinese Physical Society and IOP Publishing Ltd

beam size, implying those features smaller than the beam can be "seen".

In this paper, we are working on improving the resolution to make it below the physical limit. In order to solve the problem of the inaccuracy of the point–spread function (PSF), the complex one-shot super-resolution framework (COSSR) is put forward. This framework involves learning the THz imaging process directly from a measured reference sample and its groundtruth. This method achieves a resolution of 0.35 times wavelength, which has never been achieved before. We believe such an approach can help overcome the lower-resolution problem in THz imaging and make THz imaging more accessible and more prevalent since non-experts can still get clear images in this way. Many imaging applications, including biomedical imaging and nondestructive testing, can benefit from this approach.

2. Proposed methods

For a THz imaging system with a pixel scanning mode, considering the diffraction of the THz waves, the ideal object functions $a_{\mathrm{o}} + \mathrm{j}b_{\mathrm{o}}$ is convolution by $a_{\mathrm{PSF}} + \mathrm{j}b_{\mathrm{PSF}}$. And the measured low-resolution (LR) image $a_{\mathrm{i}} + \mathrm{j}b_{\mathrm{i}}$ is influenced by the added system noise n. Thus, the THz imaging process can be mathematically modelled by a complex two-dimensional (2D) convolution[23]

$$a_{\mathrm{i}} + \mathrm{j}b_{\mathrm{i}} = (a_{\mathrm{o}} + \mathrm{j}b_{\mathrm{o}}) * (a_{\mathrm{PSF}} + \mathrm{j}b_{\mathrm{PSF}}) + n, \tag{1}$$

where the asterisk $*$ is the convolution operation.

In practical application, the THz imaging system is affected by PSF blurring, jitter of step motor caused by moving objects, system noise, *etc*. Meanwhile, other interference information will be introduced by the measured PSF. With the increase of wavelength, less effective information can be received by the detector, and the improvement of the resolution is more limited.

Hence, the quality reduction model of the THz imaging system is obtained by the COSSR algorithm proposed in this paper, referring to learning from the mapping between a measured sample for reference and its groundtruth. This way can effectively solve the above problems.

A tailored small complex CNN (as shown in Fig. 1) is constructed to solve the THz SR task, and only a pair of data for reference needs to be provided for training. According to the framework of COSSR, the kernel dimensions of the complex convolution layers are decreased by a factor of 2 from 32 to 4. And all of the kernel sizes are set to 3×3. Instead of hoping for every few stacked layers directly to fit a desired underlying mapping, a simple residual structure is introduced to address the degradation problem. Thus, the complex convolution layers could fit a residual mapping explicitly.

Then, the image degradation process is expressed as follows:

$$\begin{aligned} &LR_{\mathrm{train}}\left(a_{\mathrm{i}} + \mathrm{j}b_{\mathrm{i}}\right) \\ &= \mathrm{Degradation-process}(\mathrm{groundtruth}_{\ \mathrm{train}}\ \left(a_{\mathrm{i}} + \mathrm{j}b_{\mathrm{i}}\right)). \end{aligned} \tag{2}$$

A relatively light complex CNN is employed and trained to reconstruct the groundtruth from its LR version:

$$\mathrm{groundtruth}_{\mathrm{train}}\left(a_{\mathrm{i}} + \mathrm{j}b_{\mathrm{i}}\right) = \mathrm{COSSR}\left(LR_{\mathrm{train}}\left(a_{\mathrm{i}} + \mathrm{j}b_{\mathrm{i}}\right)\right). \tag{3}$$

Then the desired SR image can be constructed by the map of Eq. (3). The process can be expressed as

$$SR_{\mathrm{test}}\ \left(a_{\mathrm{i}} + \mathrm{j}b_{\mathrm{i}}\right) = \mathrm{COSSR}\left(LR_{\mathrm{train}}\left(a_{\mathrm{i}} + \mathrm{j}b_{\mathrm{i}}\right)\right). \tag{4}$$

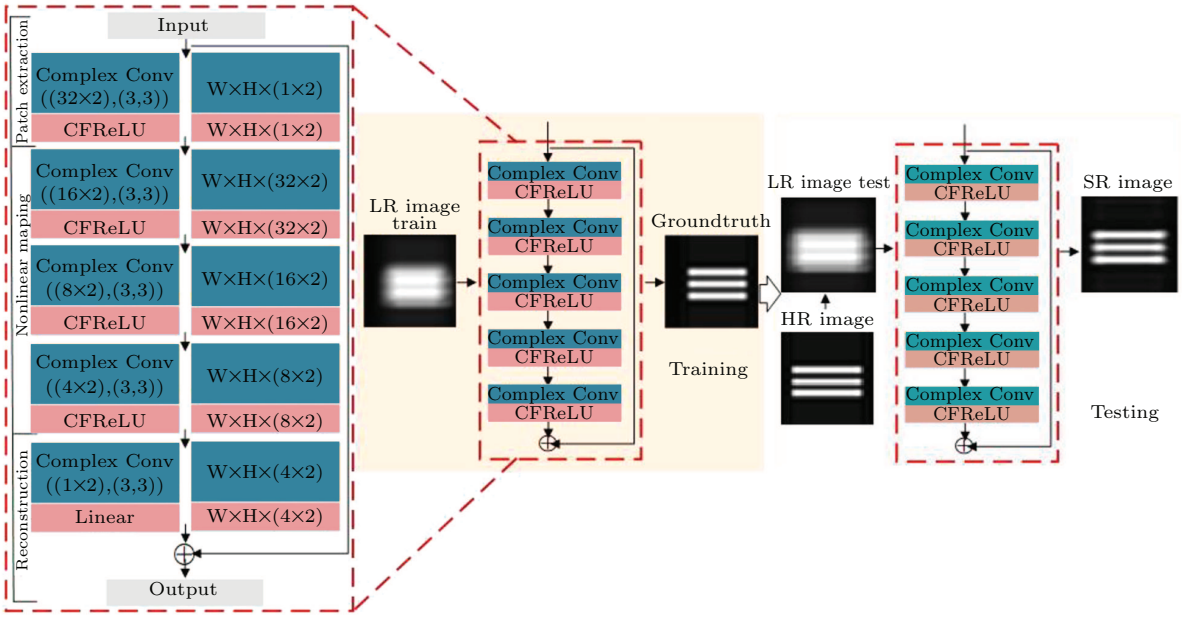


Fig. 1. The flowchart of COSSR. For a fair comparison, the frameworks of RZSSR, ROSSR, and CZSSR with five convolution layers, equivalent to COSSR, were established. The number of iterations was set as 2000 epochs. For contrasting the experiment results, the optimizer and learning rate were set to be the same.

The COSSR algorithm also can be used for different sizes of images adaptively, and the flowchart of COSSR is shown in Fig. 1. (COSSR).

The L_1 loss is chosen to optimize the COSSR:

$$L(\Theta_{\mathrm{COSSR}}) = \frac{1}{2N}\left\|\mathrm{COSSR}\left((a_{\mathrm{i}}+\mathrm{j}b_{\mathrm{i}})^{n}_{LR}\right) - (a_{\mathrm{i}}+\mathrm{j}b_{\mathrm{i}})^{n}_{\mathrm{groundtruth}}\right\|_1, \tag{5}$$

where Θ_{COSSR} represents the parameter set of COSSR.

3. Simulation analysis

The simulated LR THz image is shown in Fig. 2. We can see that the three stripes are completely aliased, which could not be distinguished. RZSSR and the edges of the restored image by CZSSR with some artifacts and ringing effects could not solve these aliased stripes. Although ROSSR obtained clear edges, the fidelity was poor. By using our proposed COSSR, the three stripes are reconstructed with clear edges, few artifacts, and ringing effects.

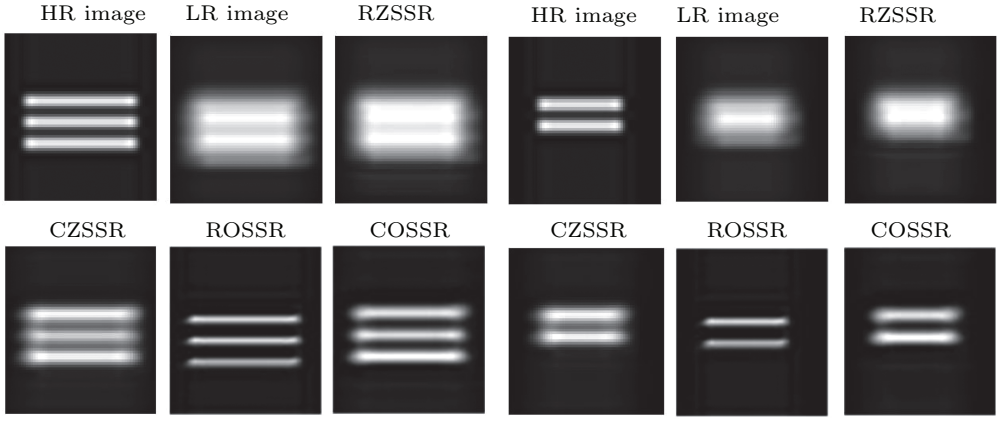


Fig. 2. Comparison of SR results of RZSSR, CZSSR, ROSSR, and COSSR. The HR image (periodical stripe image) for experiments generated by MATLAB, of which the dimension is $64 \times 64 \times 2$. And the LR image (analyzed THz image) is obtained by Eq. (1).

Additionally, the network parameters we got above were employed to verify the generalization capability of COSSR to reconstruct a similar image (two aliasing stripes) directly without any extra training. These aliased stripes still need to be solved by RZSSR, and the results of CZSSR are distorted. As previously mentioned, the SR results of ROSSR are severely distorted. And COSSR can reestablish more high-frequency information, such as the edges. The two aliasing stripes can be distinguishable easily, and the SR effect is guaranteed while the time cost is saved. Hence, we can get the conclusion that COSSR has good generalization ability.

Table 1 indicates the evaluation results, of which the best indexes of the metrics are shown in bold.

Table 1. Comparison of no-reference evaluation metrics of measured data from CCNN-T an RCNN.

	Parameters	RZSSR	CZSSR	ROSSR	COSSR
(a)	PSNR	15.2825	23.6551	14.3755	29.2591
	MSE	0.0296	0.0038	0.0365	0.0012
	SSIM	0.4610	0.8009	0.5928	0.8444
(b)	PSNR	11.9619	20.5454	11.4041	27.1315
	MSE	0.0637	0.0088	0.0724	0.0019
	SSIM	0.3427	0.7916	0.4182	0.8714

Compared with RZSSR and CZSSR, the PSNR of COSSR with three stripes aliased case, the part (a) of Table 1 improved by about 15.09 dB and 6.67 dB, MSE decreased by 0.03 and 0.003, and SSIM of it increased by 38.4% and 6.96%, respectively. And compared with ROSSR, the PSNR, MSE, and SSIM of COSSR are optimized by 17.21, 0.05, and 37.05%, separately.

As we can see in part (b) of Table 1, COSSR shows at least 6.59, 0.007, and 7.98% superior imaging efficacy in terms of PSNR, MSE, and SSIM, respectively, than other methods.

Our proposed algorithm, COSSR, obtained the best enhancement effect of the four methods, proving its validity and superiority.

4. Experiment results

As shown in Fig. 3, the THz imaging system in this paper worked at the frequency from 0.17 THz to 0.22 THz. The details of the THz imaging system components are as follows: a vector network analyzer (VNA, Keysight's N9029A) with a pair of frequency extenders (Virginia Diodes Inc., Charlottesville, VA, USA) as the transmitter and detector. And then, the VNA is connected to a host computer to collect data. Two symmetrical teflon bi-convex lenses with 100-mm diameter, 25-mm focal length (left), and 50-mm focal length (right) (taking the pupil side as an example) were applied to focus the THz beam. The object is copper with three periodic stripes with the same separation distance of 1.0 mm. The copper was moved along X and Y directions by a step motor, and both amplitude and phase can be received from transmitted waves.

By the THz imaging system mentioned in Fig. 4, wide frequency measured data is fabricated to evaluate the spatial resolution quantitatively, which is sliced into different single-

frequency to find the smallest frequency that it can recover to. Figure 4 shows that the normalized amplitude of the sample, the frequency is selected as 105 GHz. To evaluate the performance of the proposed method, the effects of RZSSR, ROSSR, and CZSSR are employed for comparison and groundtruth for reference.

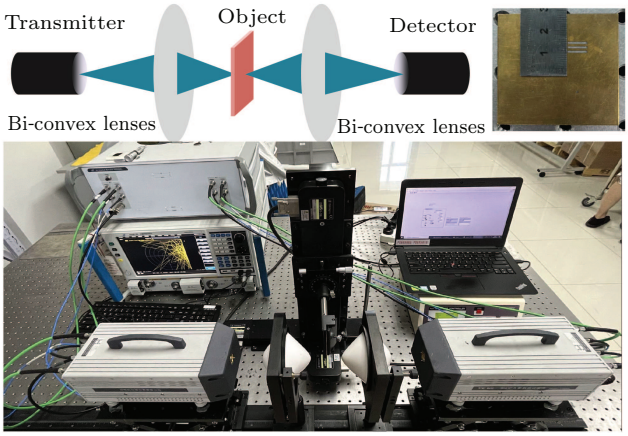


Fig. 3. Experimental setup of the THz imaging system.

The three stripes are complex aliased, which could not be distinguished. As we can see that RZSSR does not work in this aliasing case, and obvious artifacts and ringing effects were obtained by CZSSR. Compared with these two methods, ROSSR can get relatively clear SR results, but the stripes on both sides are wider than groundtruth, and the middle stripe is blurred. The result of COSSR obtained the best enhancement effect with the sharpest-edged and least artifacts than other methods. The result of our proposed method is very close to groundtruth, indicating that it has high fidelity. Furthermore, as shown in Fig. 5, we can get the same conclusion as mentioned above with the profile map of vertical amplitude. For a fair comparison, pixel values at the same location along the vertical direction are selected to show the profile map of vertical amplitude. The black dot line represents the groundtruth of the sheet copper sample with three 1-mm stripes, which can be considered as the standard reference line. Also, the line is normalized for comparison. This intuitive representation further verifies the superiority of the proposed method.

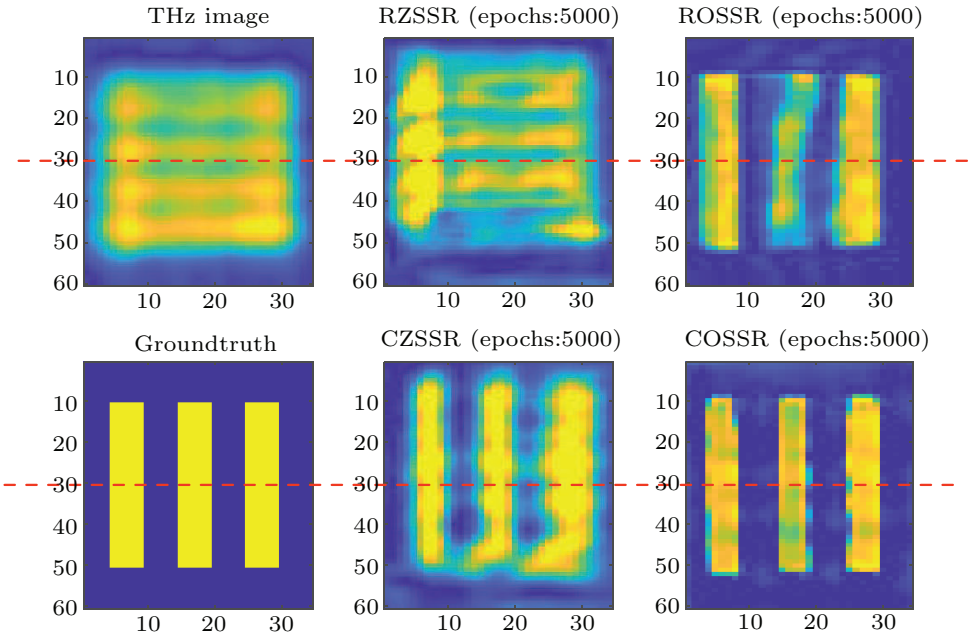


Fig. 4. The amplitude of 1-mm stripes measured from our VNA system, groundtruth for reference and, SR results of RZSSR, ROSSR CZSSR, and COSSR.

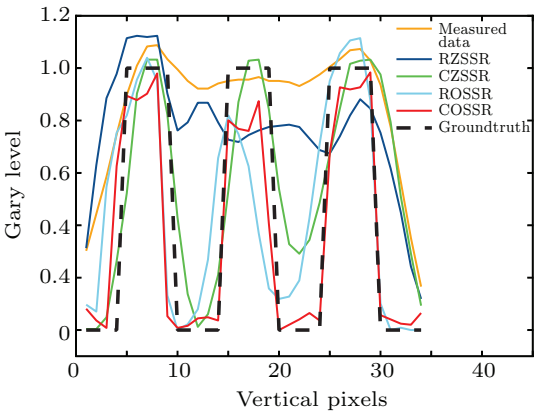


Fig. 5. Profile of the axial amplitude.

Compared with the different methods, the parameters of PSNR, MSE, and SSIM of the SR result are calculated, as introduced in Table 2. The optimal results are shown in bold. Compared with CZSSR, the PSNR of COSSR improved by about 3 dB, MSE decreased by 0.06, and SSIM increased by 14%, approximately. It means that the error between each pixel of the reconstructed image and the original image is smaller, and the SR result of COSSR has higher fidelity than CZSSR. Compared with ROSSR, the PSNR of COSSR improved by about 1.5 dB, MSE decreased by 0.025, and SSIM increased by 16%, approximately. Thus, the COSSR can reconstruct sharper and cleaner effects than ROSSR.

Table 2. Comparisons of SR performance of measured data with COSSR and ROSSR with low frequency.

Parameters	RZSSR	CZSSR	ROSSR	COSSR
PSNR	7.3670	8.9994	10.5383	11.9770
MSE	0.1834	0.1259	0.0883	0.0634
SSIM	0.1299	0.4616	0.4461	0.6001

The aliasing of three periodic stripes with the same separation distance of 1.0 mm at GHz is 0.35 times of wavelength. The ROSSR methods deal with real amplitude only. Thus, the SR performance is limited. However, as mentioned above, useful information could be extracted from the phase image to improve the resolution. It is quite feasible to gain both amplitude and phase information for complex operations in THz imaging applications. The proposed algorithm can solve the problem of complex aliased data well. The experiments show that this method can exceed the limit of diffraction resolution.

5. Conclusion

This paper presented a COSSR framework to learn the mapping directly by a reference measured sample and groundtruth. One significant advantage of the COSSR framework is it does not rely on the measured PSF. The COSSR framework reduced measurement errors and improved SR performance. In our proposed COSSR framework, a five-layer CCNN framework with a simple residual structure was applied. Weights were adaptively changed to match changes in frequency and position of THz images without prior training. A COSSR framework in the experiment demonstrated evident resolution, especially with complex aliased data, which achieved 0.35 times wavelength.

Acknowledgements

Project supported by "XingLiaoYingCai" Talents of Liaoning Province, China (Grant No. XLYC2007074), Shenyang Young and Middle-aged Science and Technology Innovation Talent Support Program (Grant No. RC200512), and the Central Guidance on Local Science and Technology Development Fund of Liaoning Province, China (Grant No. 2022JH6/100100010).

References

[1] Yan D X, Life J S and Wang Y 2019 *Acta Phys. Sin.* **68** 207801 (in Chinese)
[2] Wu J Y, Xu X F and Wei L F 2020 *Chin. Phys. B* **29** 094202
[3] Mittleman D M, Jacobsen R H and Nuss M C 1996 *IEEE J. Selec. Top. Quantum Electron.* **2** 679
[4] Chen H, Ma S H, Yan W X, Wu X M and Wang X Z 2013 *Chin. Phys. Lett.* **30** 030702
[5] Knobloch P, Schildknecht C, Kleine-Ostmann T, *et al.* 2002 *Phys. Med. Biol.* **47** 3875
[6] Joseph C S, Yaroslavsky A N, Neel V A, Goyette T M and Giles R H 2011 *Lasers in Surgery and Medicine* **43** 457
[7] Fan S, Ung B S, Parrott E P, Wallace V P and Pickwell-MacPherson E 2017 *J. Biophoton.* **10** 1143
[8] Ahi K 2017 *IEEE Trans. Terahertz Sci. Technol.* **7** 747
[9] Ahi K, Shahbazmohamadi S and Asadizanjani N 2018 *Opt. Lasers Eng.* **104** 274
[10] Karpowicz N, Zhong H, Zhang C, Lin K I, Hwang J S, Xu J and Zhang X C 2005 *Appl. Phys. Lett.* **86** 054105
[11] Quast H, Keil A and Löffler T 2010 35*th International Conference on Infrared, Millimeter, and Terahertz Waves* (IEEE) pp. 1–2
[12] Friederich F, May K H, Baccouche B, Matheis C, Bauer M, Jonuscheit J, Moor M, Denman D, Bramble J and Savage N 2018 *Terahertz Radome Inspection Photonics*, Vol. 5 (MDPI) p. 1
[13] Zhang Y, Tian Y, Kong Y, Zhong B and Fu Y 2018 *Proceedings of the IEEE Conference on Computer Vision and Pattern Recognition* pp. 2472–2481
[14] Johnson J, Alahi A and Fei-Fei L 2016 *European Conference on Computer Vision* (Springer) pp. 694–711
[15] Dong C, Loy C C, He K and Tang X 2015 *IEEE Transactions on Pattern Analysis and Machine Intelligence* **38** 295
[16] Haris M, Widyanto M R and Nobuhara H 2017 *Appl. Opt.* **56** 6043
[17] Zhang Y, Li K, Li K, Wang L, Zhong B and Fu Y 2018 *Proceedings of the European Conference on Computer Vision (ECCV)* pp. 286–301
[18] Haris M, Shakhnarovich G and Ukita N 2020 *IEEE Transactions on Pattern Analysis and Machine Intelligence* **43** 4323
[19] Long Z, Wang T, You C, Yang Z, Wang K and Liu J 2019 *Appl. Opt.* **58** 2731
[20] Li Y, Hu W, Zhang X, Xu Z, Ni J and Ligthart L P 2020 *Opt. Express* **28** 22200
[21] Han Z, Hu W, Li Y, Xu Z, Zhao Y, Ni J and Ligthart L 2020 *Cross Strait Radio Science & Wireless Technology Conference (CSRSWTC) (IEEE)* pp. 1–3
[22] Ning W, Qi F, Liu Z, Wang Y, Wu H and Wang J 2019 *IEEE Access* **7** 65116
[23] Wang Y, Qi F and Wang J 2021 *Opt. Lett.* **46** 3123
[24] Wang Y, Qi F and Wang J 2022 *Appl. Opt.* **61** 5831